*Macromol. Symp.* ***181,*** *289–301 (2002)*

# Potential of Recent Rubber-Elasticity Theories for Describing the Tensile Stress-Strain Dependences of Two-Phase Polymer Networks

*Bohumil Meissner**, *Milena Špírková*

Institute of Macromolecular Chemistry, Academy of Sciences of the Czech Republic, Heyrovský Sq. 2, 162 06 Prague 6, Czech Republic

**Summary**: The potential of recent rubber-elasticity theories for giving a well-founded, molecularly based and as-precise-as-possible description of experimental tensile stress-strain dependences of two-phase polymer networks (such as block polymers of the polyurethane and styrene-butadiene-styrene type) up to the break has been explored. Theoretical arguments lead to the conclusion that the rigorous theory of the high-strain hardening effect based on Langevin statistics (Arruda and Boyce, 1993) is to be preferred to the slip-link and extended-tube theories in view of the approximations involved in their derivation. None of the existing theoretical treatments of the low-strain softening was found suitable for the purpose of the study. Therefore, a semiempirical solution had to be chosen by combining the Langevin-theory-based term with an empirically modified $C_2$ term of the Mooney-Rivlin equation, similarly to the treatment used previously for unfilled and filler-reinforced networks (Meissner and Matějka, 2000, 2001). A very good data description is obtained for networks with different contents of hard blocks, up to 50 %, provided that yield does not appear. The parameter values of the proposed equation have been determined for a number of two-phase networks and their relations to structural parameters are discussed. The experimental high-strain behavior strongly suggests the presence (absence) of topological changes on increasing (decreasing) elongation, of the same kind as observed previously for unfilled and filler-reinforced networks. Thus, a unified picture of the tensile stress-strain behavior of rubbery networks of all kinds emerges.

## Introduction

The experimental tensile stress-strain behavior of real rubber-like networks deviates from the classical Gaussian theory (cf. Treloar[1]) in two important respects. At low strains, the reduced tensile stress $\sigma_{\text{red}} = \sigma/(\lambda - 1/\lambda^2)$ decreases with increasing stretch ratio, $\lambda$ ($\sigma$ is the nominal tensile stress, i.e. force per unit area of undeformed cross-section, and $(\lambda - 1/\lambda^2)$ is the function calculated in the Gaussian theory). This phenomenon is referred to as low-strain softening and is generally ascribed to some kind of constraints which restrict free mobility of network junctions and chains. The

CCC 1022-1360/00/$ 17.50+.50/0

constraint contribution to the stress increases with increasing strain at a lower rate than the stress predicted by the Gaussian theory and this leads to a decrease in reduced stress. In the region of high strains, the experimental reduced stress is generally found to increase with increasing stretch ratio (high-strain hardening). A theoretical explanation of the high-strain hardening effect, based on the idea of finite (limiting) extensibility of network chains and modelled by the Langevin chain statistics, was offered already in the forties and tensile stress-strain dependences were calculated by James and Guth.[2] A more rigorous Langevin-type theory which gives a reasonable prediction of the stress-strain dependences for different deformation modes, was given by Arruda and Boyce.[3] Their treatment is to be preferred to the slip-link and extended-tube theories[4,5] in view of the approximations that the latter theories introduce when modelling the high-strain singularity in entropy. It should be noted that the predictions of the tensile behavior given by the theories of James and Guth on one hand and by Arruda and Boyce on the other differ but marginally if the two parameters of the respective equations are suitably adjusted.[6]

A number of molecular theories of the low-strain softening effect have been published (cf. Erman, Mark[7]) which, however, do not attempt at modelling the high-strain behavior. Recently, Boyce and Arruda[8] have combined the Flory-Erman constrained junction theory of low-strain softening with the Arruda-Boyce theory of high-strain hardening in an attempt to obtain a satisfactory description of the well-know Treloar uniaxial and biaxial data up to high strains;[1] however, the result has not been successful. Following their approach, we have similarly tested other theories of the low-strain softening but the results have generally been unsatisfactory as well.[9]

In our previous papers[6,10,11] we have come to the conclusion that for tensile stress-strain dependences of both unfilled and filler-reinforced networks, the requirement of an as-precise-as-possible data description can be satisfactorily met by an equation which we denote by the JGmC2 code. It combines the result of the molecular theory of James and Guth with a phenomenological part which is given by the C2 term of the Mooney-Rivlin equation[12,13] modified by the introduction of a further adjustable parameter, $n$ :

$$\sigma = 2\, C_1\, (\lambda_m/3)\, [L^{-1}(\lambda/\lambda_m) - (1/\lambda^{3/2})\, L^{-1}(1/\lambda^{1/2}\lambda_m)] + 2\, C_2\, (1 - 1/\lambda^{3n}) \qquad (1)$$

$L^{-1}$ is the inverse Langevin function ($L(x) = \coth(x) - 1/x$ is the Langevin function); $C_1$, $C_2$, $\lambda_m$, $n$ are the four parameters of the JGmC2 equation. In the James-Guth theory, $2C_1$ is the modulus which in the phantom Gaussian theory[7] is predicted to depend on the concentration, $C$, and functionality, $f$, of network junctions: $2C_1 = C\,R\,T\,(f - 2)/2$; $\lambda_m$ is the finite (or limiting) extensibility parameter (the hypothetical highest possible stretch ratio), which is predicted to be given by the square root of the number, $Z$, of statistical segments in the network chain: $\lambda_m = Z^{1/2}$; $2C_2$ is the limiting value of the constraint term at high tensile strains; $n$ reflects the degree of curvature of the stress-strain dependence at low strains. The JGmC2 equation includes the following special cases: the James-Guth equation ($C_2 = 0$); the modified Mooney-Rivlin equation ($\lambda_m \rightarrow \infty$); the Mooney-Rivlin equation ($\lambda_m \rightarrow \infty$, $n = 1$); the Gaussian equation ($C_2 = 0$, $\lambda_m \rightarrow \infty$).

The JGmC2 equation shows a surprisingly good flexibility for a precise description (less than 5 % deviation) of tensile data at low and medium strains. In the region of high strains, the JGmC2 equation gives a good fit to tensile data recorded on *decreasing* elongation.[10] On the other hand, comparison of the JGmC2 equation with stress-strain dependences obtained in the usual way, i.e., on increasing elongation, shows that at high strains, the experimental stress increases less steeply than predicted by the JGmC2 equation.[6,10,11] We have ascribed this phenomenon to topological changes which are induced by increasing strain; they are assumed to lead to an increase in the network mesh size and, thus, to an increase in the finite extensibility parameter. The dependence of $\lambda_m$ on $\lambda$ can be obtained from a comparison of experimental data with the JGmC2 equation[6] and described by the following power function with parameters $\lambda_1$, $\lambda_2$, $\lambda_{m,1}$, $\lambda_{m,2}$, $a$ (only three of them being adjustable[6,11]):

$$\lambda \leq \lambda_1: \qquad \lambda_m = \lambda_{m,1}$$

$$\lambda > \lambda_1: \qquad \lambda_m = \lambda_{m,1} + (\lambda_{m,2} - \lambda_{m,1}) \left[ (\lambda - \lambda_1) / (\lambda_2 - \lambda_1) \right]^a \tag{2}$$

The JGmC2 equation with a $\lambda$-dependent finite extensibility parameter is designated here by the JGmC2L code; it is given by equations (1) and (2). Conclusions based on a comparison of the JGmC2L equation with the stress-strain behavior of filler-reinforced networks were summarized previously.[10,11]

In the present paper the JGmC2L approach is applied to the tensile stress-strain behavior of hard-domain reinforced rubbery networks.

## Experimental

Experimental data on the systems given below were used for a representative comparison with the JGmC2L equation. If not stated otherwise, stress-strain measurements were performed at room temperature using a strain rate around 0.03/s.

(1) Polybutadiene urethane, PBUR

Networks were synthesized in the way described previously (Špírková et al.[14]). Soft segments: polybutadiene diol (1,2 addition 60%, 1,4-trans 25%, 1,4-cis 15%). The hard-segment content HSC is 35%. Chemical crosslinking was achieved using a cyclotrimerization reaction, concentration of crosslinks is 60 mol/m$^3$. Stress-strain data were obtained by us.

(2) Polyester urethane, PEUR

Synthesized and stress-strain behavior studied by Furukawa et al.[15] Soft segments: aliphatic polyester. Hard segment content and allophanate crosslinking are variable. Low strain rate at 50 °C.

(3) Polyether (urethane-urea), PEUUR

Synthesized and stress-strain behavior studied by Trick.[16] Soft segments: aliphatic polyether. HSC 18% , aromatic diamine, excess of isocyanate groups.

(4) Polyether (urethane-urea), PUUR RIM

Synthesized and stress-strain properties studied by Ryan et al.[17] Soft segments: aliphatic polyether with chemical crosslinks. HSC 50%. The system is used for the RIM technology.

(5) Low-crystallinity copolymers of ethylene and octene, PEO

Prepared using the constrained geometry catalyst, measured by Bensason et al.[18] Octene content 12.3 mol %, degree of crystallinity 12% at room temperature.

(6) Styrene - butadiene - styrene teleblock copolymer, SBS

30% of styrene, measurements at different temperatures done by Smith and Dickie.[19]

(7) α-Methylstyrene - isoprene - α-methylstyrene teleblock copolymer, mSImS

α-Methylstyrene content 33 %. Measured by Fetters and Bi.[20]

(8) Styrene - isoprene nine-arm star teleblock copolymer, (SI)9

Styrene content 28%. Measured by Fetters and Bi.[20]

Using literature data, experimental points were read off from magnified graphs.

## Results and Discussion

Low-strain experimental data obtained by Furukawa et al.[15] on polyester urethanes under quasi-equilibrium conditions are shown in Figure 1 (points) in the Mooney-Rivlin plot (reduced stress vs. reciprocal stretch ratio). The content of hard segments and the concentration of allophanate crosslinks increase in the series from curve 1 to 3 (in the original paper,[15] the three networks are designated N2M6, T3M6, H3M4). As is apparent, the curves drawn according to the modified Mooney-Rivlin equation

(equation (1) with $\lambda_m \rightarrow \infty$; parameters in Table 1) are able to describe the data very well. It should be noted that slightly different values of parameters $n$, $C_1$, $C_2$ are obtained from a comparison of the JGmC2L equation with experimental data which include measurements up to high strains.

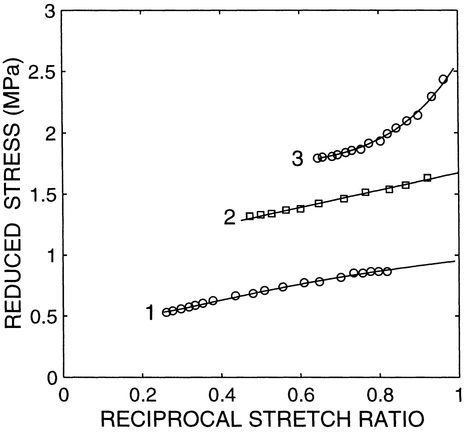

Figure 1. Points: experimental stress-strain data on polyester urethanes in the Mooney-Rivlin coordinates. Curves are drawn according to the modified Mooney-Rivlin equation for parameter values given in Table 1.

Table 1. Parameters of the modified Mooney-Rivlin equation for polyester urethane curves given in Figure 1.

| | 1 | 2 | 3 |
|---|---|---|---|
| $n$ | 0.75 | 1.0 | 5.0 |
| $C_1$ (MPa) | 0.15 | 0.483 | 0.80 |
| $C_2$ (MPa) | 0.46 | 0.355 | 0.10 |

The stress-strain behavior on recovery and repeated extension was explored using a polybutadiene urethane network. The results are given in Figures 2, 3 and in Table 2. The quasi-permanent deformation (tensile set TS) measured after recovery from prestrain (pre-stretch ratio $\lambda_p$) of a polybutadiene urethane is generally higher than that of the carbon black-reinforced styrene-butadiene networks;[10,11] this may be due to a less perfect network structure of the polybutadiene urethane. In both types of network, prestraining leads to a significant reduction in the parameter $n$, which can be ascribed to a decreased interconnectivity of filler particles and hard-domain particles. On retraction, both $C_1$ and $C_2$ are distinctly lower than on the first extension; $C_2$ seems to have recovered slightly for the second extension while $C_1$ retains a lower value. For stretch ratios smaller than $\lambda_p$, the finite extensibility parameter $\lambda_m$ assumes a value which lies but slightly above the pre-stretch ratio $\lambda_p$ (more precisely, slightly above ($\lambda_p$ - TS)) and

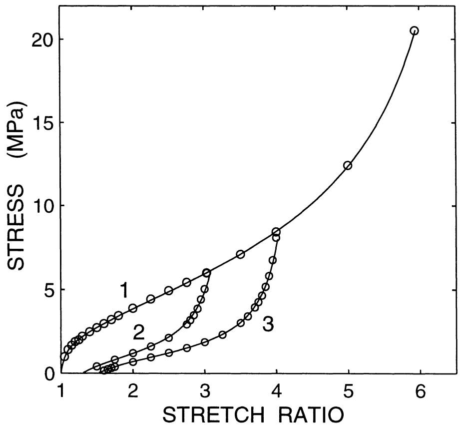

Figure 2. Polybutadiene urethane. Points: experimental. Curves are drawn according to the JGmC2L equation for parameter values given in Table 2. 1 - first extension; 2 - retraction after prestrain to stretch ratio $\lambda_p = 3$; 3 - retraction after prestrain to $\lambda_p = 4$.

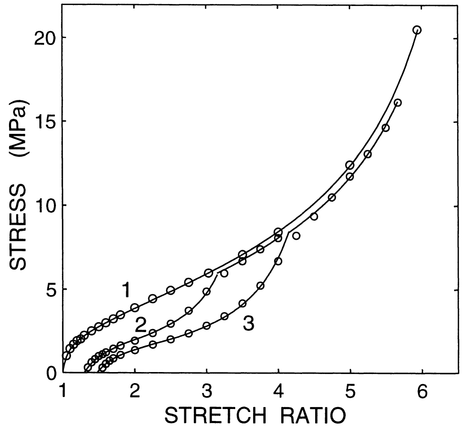

Figure 3. Polybutadiene urethane. Points: experimental. Curves are drawn according to the JGmC2L equation for parameter values given in Table 2. 1 - first extension. 2 - second extension after prestrain to $\lambda_p = 3$; 3 - second extension after prestrain to $\lambda_p = 4$.

Table 2. Parameter values of the JGmC2L equation for a polybutadiene urethane network (curves in Figures 2 and 3).

| | 1st extension | retraction | | 2nd extension | |
|---|---|---|---|---|---|
| $\lambda_p$ | | 3 | 4 | 3 | 4 |
| $n$ | 6.5 | 1.0 | 1.0 | 1.2 | 1.5 |
| $C_1$ (MPa) | 0.74 | 0.33 | 0.26 | 0.20 | 0.255 |
| $C_2$ (MPa) | 0.56 | 0.02 | 0.06 | 0.70 | 0.42 |
| $\lambda_1$ | - | - | - | 2.10 | 2.40 |
| $\lambda_{m1}$ | 7.30[a)] | 3.14[a)] | 3.82[a)] | 2.80 | 3.55 |
| $\lambda_2$ | 5.94 | 3.00 | 4.00 | 3.00 | 4.00 |
| $\lambda_{m2}$ | 7.30[a)] | 3.14 | 3.82 | 3.22 | 3.97 |
| $a$ | - | - | - | 1.20 | 1.35 |
| TS | 0 | 0.30[b)] | 0.50[b)] | 0.30[c)] | 0.45[c)] |

[a)] $\lambda_{m2} = \lambda_{m1}$, i.e., $\lambda_m$ does not change with $\lambda$. [b)] TS measured immediately after retraction.
[c)] TS measured after 5 min relaxation before beginning of the second extension.

is thus smaller than that found on the first extension. For the evaluation of the JGmC2L parameters from data with tensile set, see references.[6,10] For $\lambda$ larger than $\lambda_p$, the stress-strain dependence and the finite extensibility parameter are little affected by prestraining (Figure 3). While on retraction $\lambda_m$ is practically constant, on subsequent second extension it shows a tendency to increase with $\lambda$ (Table 2). All these effects are also observed in filler-reinforced networks.[10,11]

Three polyurethane networks widely differing in their stress-strain behavior are compared in Figure 4 in linear coordinates and in Figure 5 in coordinates log(reduced stress) vs. stretch ratio. The parameter values are given in Table 3. The PEUUR RIM network contains a high fraction of hard domains which are obviously highly interconnected. This leads to a yield-like behavior which is reflected in very high values of $n$ and $C_2$. The high value of $C_1$ apparently reflects the presence of crosslinks in the rubbery matrix and a contribution from the hard domain - matrix interphase. The polyether (urethane-urea) shows a pronounced high-strain hardening (curves 2 and 3 in Figures 4 and 5) which is accompanied by a significant increase in the finite extensibility parameter from 4.1 to 6.11. On second extension, the corresponding change is much smaller, ranging from 5.75 to 6.11. The stress-strain behavior of a polyester urethane (curve 4 in Figures 4 and 5) was measured at a very slow rate of strain and at an increased temperature. Its stress-strain behavior approaches the JGC2 type, with the parameter $n$, however, being smaller than unity and with the $C_2/C_1$ ratio of 4 still being rather high, although smaller than that of the other two networks - around 10. Figure 5 documents the advantage of the log(reduced stress) vs. stretch ratio plot; the relative point-curve deviations and the differences in the low-strain reduced stress amounting to a factor of 100 are clearly seen.

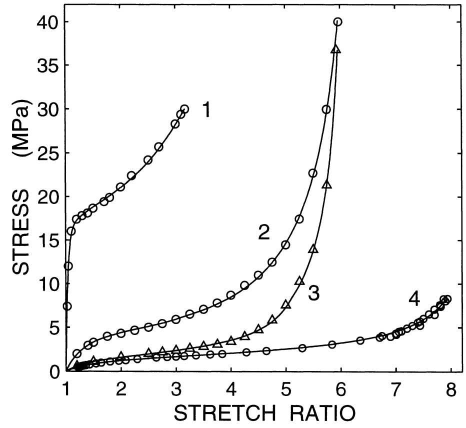

Figure 4. Points: experimental.[15-17] Curves: drawn according to the JGmC2L equation for parameter values given in Table 3. 1 - PEUUR RIM, 1st extension; 2 - PEUUR, 1st extension, 3 - PEUUR, 2nd extension after prestrain to $\lambda = 6$; 4 - PEUR, 1st extension.

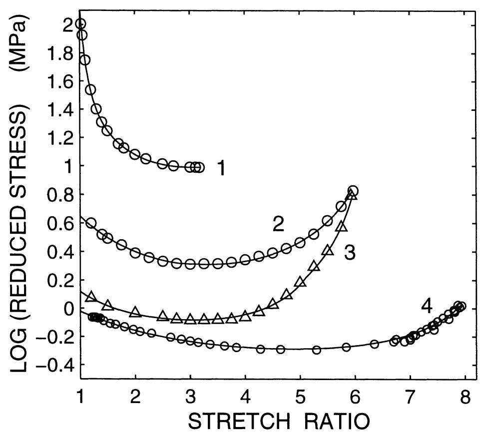

Figure 5. For legend, see Figure 4.

Table 3. Parameter values for curves in Figures 4 and 5.

| | PEUUR RIM | PEUUR | | PEUR |
|---|---|---|---|---|
| | | 1st extension | 2nd extension | (at 50 °C) |
| $n$ | 8.0 | 1.0 | 1.0 | 0.70 |
| $C_1$ | 0.80 | 0.21 | 0.22 | 0.125 |
| $C_2$ | 8.20 | 2.01 | 0.43 | 0.50 |
| $\lambda_1$ | 1.50 | 3.05 | 5.10 | - |
| $\lambda_{m1}$ | 2.60 | 4.10 | 5.75 | 8.80 |
| $\lambda_2$ | 3.17 | 5.97 | 5.96 | 7.94 |
| $\lambda_{m2}$ | 3.70 | 6.11 | 6.11 | 8.80 |
| $a$ | 1.20 | 1.12 | 1.20 | - |

The effect of increasing temperature on the stress-strain dependence of the SBS triblock copolymer (Figure 6, Table 4) is manifested by a decrease in the modulus components $C_1$, $C_2$ and in an increase in the finite extensibility. Surprisingly, parameter $n$ is practically independent of the temperature of measurement. The $C_2/C_1$ ratio of the given SBS network (around 10) is large but comparable to a single-phase network based on a styrene-butadiene random copolymer crosslinked with a small number of chemical

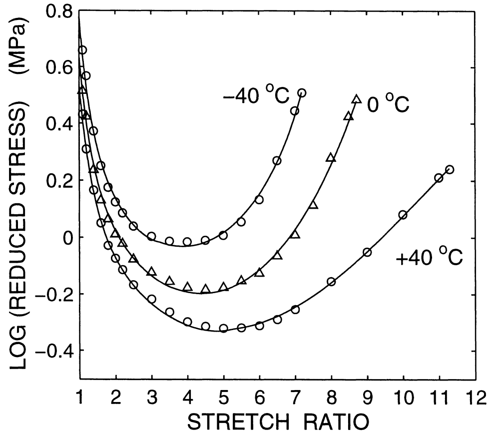

Figure 6. Polymer: SBS. Points: experimental.[19] Curves are drawn according to the JGmC2L equation for parameter values given in Table 4.

Table 4. Parameter values for curves in Figures 6 and 7.

| | SBS, -40 °C | SBS, 0 °C | SBS, +40 °C | mSImS | (SI)9 |
|---|---|---|---|---|---|
| $n$ | 2.9 | 2.7 | 2.7 | 1.80 | 1.25 |
| $C_1$ | 0.095 | 0.078 | 0.068 | 0.36 | 0.20 |
| $C_2$ | 1.01 | 0.78 | 0.62 | 1.12 | 0.615 |
| $\lambda_1$ | 3.23 | 3.70 | 5.20 | 4.00 | 9.00 |
| $\lambda_{m1}$ | 4.45 | 5.65 | 7.07 | 5.70 | 10.70 |
| $\lambda_2$ | 7.20 | 8.72 | 11.30 | 10.10 | 11.50 |
| $\lambda_{m2}$ | 7.36 | 8.88 | 11.60 | 10.65 | 11.95 |
| $a$ | 1.11 | 1.34 | 1.23 | 1.18 | 1.73 |

crosslinks.[11] A contribution to $C_2$ from the hard domain - matrix interphase also plays a role, as evidenced by our unpublished results which indicate an increase in $n$ and $C_2$ with increasing content of styrene in SBS. This is analogous to the increase in $n$ and $C_2$ with increasing filler loading observed previously in filler-reinforced networks.[11]

The high-strain behavior of a radial nine-arm block copolymer of isoprene and styrene shows a much smaller strain dependence of the finite extensibility parameter than does that of SBS and mSImS linear triblock copolymers (Figure 7). The reason for this behavior is not clear at present.

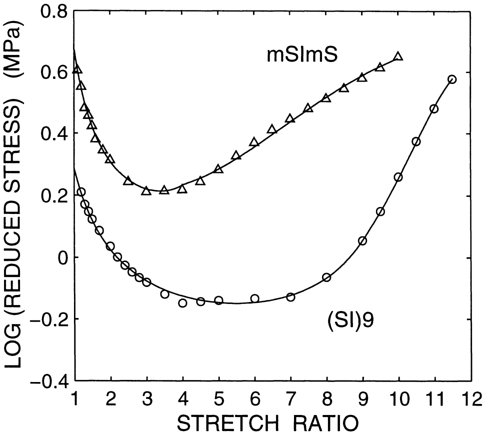

Figure 7. Points: experimental.[20] Curves are drawn according to the JGmC2L equation for parameter values given in Table 4.

Low-crystallinity copolymers of ethylene and octene show a long-range elasticity provided the length of polymer chains and the functionality and number of crystallites (i.e., polyfunctional network junctions) satisfy the requirement for the formation of a continuous network. For the copolymer with 12.3% of octene and $M$=57 kg/mol,[18] this is obviously fulfilled both at 0 °C and 40 °C (curves 1, 2 in Figure 8, parameters in Table 5). With increasing temperature of measurement, $n$, $C_1$, $C_2$ decrease, the extensibility increases and the phenomenon of high-strain hardening becomes less pronounced. If $M$ of the copolymer is decreased to 32 kg/mol, then at 40 °C the network connectivity probably decreases close to the gel-point and the high-strain hardening effect disappears.[18] Instead, a high-strain softening - in addition to the low-strain one - is observed. Curve 3 in Figure 8 shows that such an effect can be modelled by the JGmC2L equation with a reasonable accuracy. Compared to the SBS network, the ethylene-octene copolymer shows a more significant decrease in $C_2$ with increasing temperature. In the 0 °C to 40 °C range, the degree of crystallinity of the ethylene-octene copolymer decreases while the fraction of hard polystyrene domains in the SBS copolymer can be expected not to change much. This again suggests that $C_2$ of two-phase networks receives a significant contribution from the hard domain - matrix interphase.

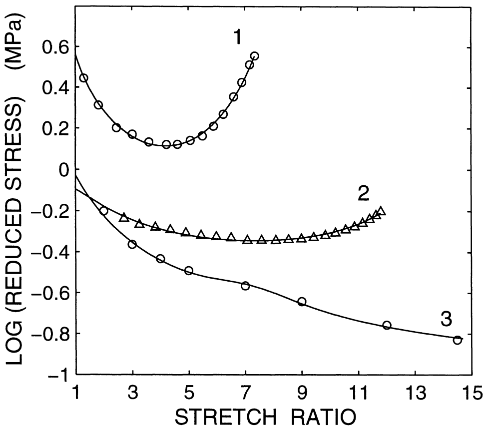

Figure 8. Low-crystallinity copolymers of ethylene and octene. Points: experimental.[18] Curves are drawn according to the JGmC2L equation for parameter values given in Table 5.

Table 5. Parameters of the JGmC2L equation for PEO curves in Figure 8.

| Curve | 1 | 2 | 3 |
|---|---|---|---|
| $M$ (kg/mol) | 57 | 57 | 32 |
| $T$ (°C) | 0 | 40 | 40 |
| $n$ | 1.10 | 0.50 | 0.75 |
| $C_1$ | 0.18 | 0.13 | 0.035 |
| $C_2$ | 1.50 | 0.54 | 0.58 |
| $\lambda_1$ | 3.90 | - | 5.00 |
| $\lambda_{m1}$ | 5.84 | 14.90 | 8.90 |
| $\lambda_2$ | 7.35 | 11.80 | 14.50 |
| $\lambda_{m2}$ | 7.65 | 14.90 | 70 |
| $a$ | 1.40 | - | 2.70 |

## Conclusion

The tensile stress-strain behavior of two-phase hard-domain-reinforced polymer networks can be described with a sufficient degree of accuracy in the whole strain range up to break with the use of the JGmC2L equation. It is a combination of the molecular James-Guth equation and a modified C2 term of the Mooney-Rivlin equation and is based on the concept of topological changes induced by high increasing strains. On decreasing strain, such changes have been found to be essentially absent. Parameters of the JGmC2L equation were determined for a number of two-phase hard-domain-reinforced networks (multiblock networks of the polyurethane and poly(urethane-urea) type, linear and radial teleblock polymers of the styrene-butadiene type and low-crystallinity polyolefins) and their relation to structure is discussed. The tensile stress-strain behavior of the explored hard-domain-reinforced networks shows essentially the same features as that of filler-reinforced networks. Differences are a matter of degree rather than kind. Thus, a unified picture of the tensile stress-strain behavior of rubbery networks of all kinds emerges.

**Acknowledgement.** The authors are greatly indebted to the Grant Agency of the Czech Republic for the financial support within the grant project No. 104/00/1311.

[1] L. R. G. Treloar, "*The Physics of Rubber Elasticity*", 3rd ed., Clarendon Press, Oxford 1975.
[2] H. M. James, E. J. Guth, *J. Chem. Phys.* **1943,** *11*, 455.
[3] E. M. Arruda, M. C. Boyce, *Mech. Phys. Solids* **1993**, *41*, 389.
[4] S. F. Edwards, T. A. Vilgis, *Polymer* **1986**, *27*, 483.
[5] M. Kaliske, G. Heinrich, *Rubber Chem. Technol.* **1999**, *72*, 602.
[6] B. Meissner, *Polymer* **2000**, *41*, 7827.
[7] B. Erman, J. E. Mark, *"Structure and Properties of Rubberlike Networks"*, Oxford University Press, New York 1997.
[8] M. C. Boyce, E. M. Arruda, *Rubber Chem. Technol.* **2000**, *73*, 504.
[9] B. Meissner, L. Matějka, to be published
[10] B. Meissner, L. Matějka, *Polymer* **2000**, *41*, 7749.
[11] B. Meissner, L. Matějka, *Polymer* **2001**, *42*, 1143.
[12] M. Mooney, *J. Appl. Phys.* **1940**, *11*, 582.
[13] R. S. Rivlin, *Philos. Trans. R. Soc.* **1948,** *A241*, 379.
[14] M. Špírková, L. Matějka, D. Hlavatá, B. Meissner, J. Pytela, *J. Appl. Polym. Sci.* **2000,** *77*, 381.
[15] M. Furukawa, M. Komiya, T. Yokoyama, *Angew. Makromol. Chem.* **1996**, *240*, 205.
[16] G. S. Trick, *J. Appl. Polym. Sci.* **1960**, *3*, 252.
[17] A. J. Ryan, J. L. Stanford, R. H. Still, *Polymer* **1991**, *32*, 1426.
[18] S. Bensason, E. V. Stepanov, S. Chum, A. Hiltner, E. Baer, *Macromolecules* **1997**, *30*, 2436.
[19] T. L. Smith, R. A. Dickie, *J. Polym. Sci.* **1969**, *C26*, 163.
[20] L. J. Fetters, K. L. Bi, *Rubber Technol. Conf.* Tokyo **1975,** I-3-04.